Optimizing the Use of Surface Sensors for Wind Shear Detection

A J Bedard Jr *
NOAA/ERL, Boulder, Colorado

Optimizing the use of surface sensors for wind shear detection involves addressing a broad range of physical processes and time and spatial scales, in addition to the operational considerations of providing timely warnings with systems that are practical to install and maintain Concentrating on thunderstorm gust fronts and down bursts important properties for detection and warning are reviewed from the perspectives of both analytical calculations and experimental measurements Calculations of such properties as the forms of the low level divergence fields and dynamic pressure changes indicate important measurement scales for the use of combined sensing systems of anemometers and pressure sensors

Nomenclature

N	= constant determining the variation of W from the center of the jet
r	= radial distance from center of downflow
R	= maximum radius of downflow at source region
W	= vertical wind speed
W_{max}	= vertical wind speed at source region
Z	= vertical height above the surface of the Earth
Z_{max}	= vertical height of the source region
σ	= characteristic width
ρ	= air density

Introduction

THE Low Level Wind Shear Alert System (LLWSAS) was deployed by the Federal Aviation Administration as a method of detecting wind shear related to large scale thun derstorm gust fronts [1] Although this system is well conceived and executed for the detection of such cold air outflows, improvements are possible (e g., earlier warning times) through the application of pressure sensors In addition other aspects of the wind shear hazard (e g , gravity/shear waves, orographic flows, and concentrated downflow regions) can require additional or specialized detection methods [2] The following sections review the physical properties of some of these hazards and discuss features that are important from the perspective of optimizing detection using surface sensors

Thunderstorm Outflows

Low level wind shear events are often accompanied by large and abrupt pressure changes Thus pressure sensor arrays provide a useful complement to wind sensor arrays Charba[3] described the sequence of events associated with the passage of the leading edge of a cold air outflow from a thun derstorm He found that such transition regions were characterized initially by a wind shift line, typically followed in order by a pressure jump line, gust surge line, and tem perature drop line He noted that these outflow systems often moved at speeds faster than predicted from a simple gravity current model and suggested that an important consideration for many of these systems is the long term provision of energy from the source region Charba's observations describe a frequent sequence of events providing guidance for the ap plication of surface sensors

Bedard et al [4] also found that the pressure jump line frequently precedes the gust surge Figure 1 shows a typical example, taken from an experiment at O'Hare Airport; Fig. 2 summarizes statistics illustrating this point A physical ex planation exists for the arrival of the pressure jump line prior to the wind surge line The upward acceleration of the streamlines before the arrival of the temperature discontinuity is associated with a pressure rise Wakimoto[5] came to a similar conclusion This pressure rise can be estimated by using a source in a potential flowfield The stagnation pressure at the leading edge can be estimated for various speeds of motion and compared with the hydrostatic pressure field from the head of colder air Figure 3 illustrates that under some conditions the dynamic pressure field at the leading edge can be larger than the hydrostatic field This increased pressure can be expected to occur for energetic density currents driven in part by source region energy and give warnings of the arrival of the density current Warnings in excess of 2 min can be provided It is important to take advantage of this warning potential especially when the parallel problems posed by the need for rapid data dissemination are also considered Table 1 reviews the effects from large scale thunderstorm outflows

Thunderstorm Microbursts

In contrast with large scale thunderstorm outflows, small scale microburst events produce a series of different near surface effects Although concentrated downflows have only

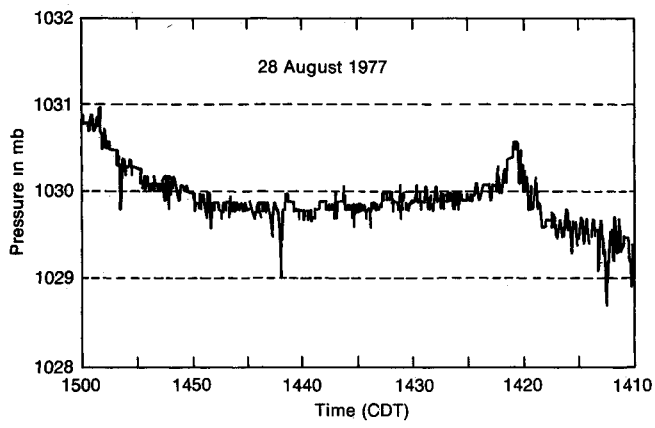

Fig 1 Example of a pressure jump recorded at O'Hare Airport

Presented as Paper 84 0353 at the AIAA 22nd Aerospace Sciences Meeting Reno Nev Jan 9 12 1984; received April 18 1984; revision received July 30 1984 This paper is declared a work of the U S. Government and therefore is in the public domain

*Physicist Wave Propagation Laboratory Member AIAA

recently been identified as an important meteorological entity and an aircraft hazard,[6] in retrospect microburst effects can be found reported in the older meteorological literature For example, Faust[7] describes the occurrence of a gust surge and pressure nose associated with straight-line and small scale damage patterns now known to be characteristic of microbursts Although much remains to be learned about the generation mechanisms and dominant physical processes, several recent experiments provide examples of near-surface effects accompanying microbursts Some of these effects appear in Table 2 Many of these general comments result from a review of microburst cases identified during the Joint Airport Weather Studies (JAWS) Project However there are few measurements within the impact region of a microburst

Bedard et al [4] provide an example (Fig 4) of the abrupt and complex wind vector changes that can occur in the microburst impact region A large pressure nose (Fig 5) also ac companied this event Paradoxically, only minor wind speed changes may accompany the direct impact of a microburst on an anemometer site (since it can be at a stagnation point) An increase in pressure will probably be the first surface effect, but little is known about the phase relationships in the source region, since measurements with sufficient time resolution are not available The dynamic pressure rise at the surface should begin when the leading edge of the downflow is at a height above the surface approximately equal to the diameter Lead times of 100 200 s are possible

Also, at distances from the source region, apparently in excess of the microbursts diameter, only minor pressure changes are observed This reflects the fact that outflows of only limited heights (e g , <300 ft) may occur and, in some cases, the hydrostatic effects seem only minor Positive (or no changes) as well as negative temperature changes have been observed Thus, while pressure sensors seem well suited for detection in the microburst impact region, they do not seem suited for the regions of the diverging flow outside the core region In these outer regions, the sudden appearance of a large gust surge may be the best indicator The abruptness of the wind speed changes may serve as the basis of a detection algorithm The rapid onset time also emphasizes the need for rapid information transfer

Since there are numerous case studies in the literature describing thunderstorm gust fronts, it seems surprising that equivalent downflow documentation does not exist Part of

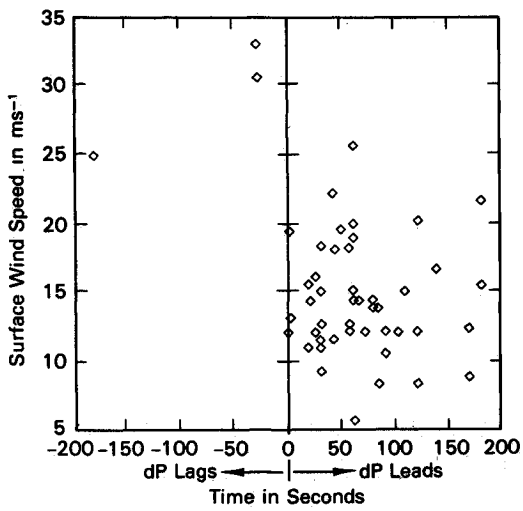

Fig 2 Data illustrating the relative arrival times of pressure jumps relative to the gust surge lines

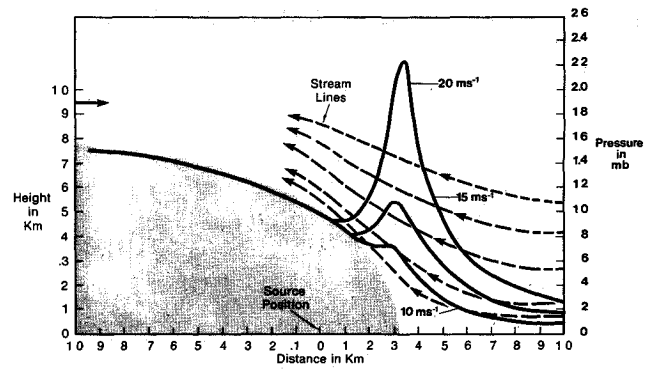

Fig 3 Potential flow source in a uniform flowfield used to illustrate the physical process causing the early arrival of the pressure increase

Table 1 Near surface effects from large scale thunderstorm outflows

Pressure	Pressure jumps in excess of 1 mb over 5 min often accompany the leading edge of the discontinuity; pressure jumps usually precede the gust surge
Wind speed	A range of wind speed changes of 0 60 knots can accompany the frontal region with the stronger surges usually accompanying the larger wind vector changes
Wind direction	A wind shift line precedes other effects; shifts from inflows to outflows of 180 deg often occur
Temperature	A temperature drop is usually the last effect to be clearly represented; decreases in the range of 5 10°C are typical for the strongest events

Table 2 Microburst near surface effects

	Impact region	1 2 km from edge
Pressure	Large pressure nose	Little or no pressure change (in some cases a decrease)
Wind speed	No change or abrupt surge	Abrupt surge
Wind direction	Complex direction change	Abrupt direction change often followed by a grad ually veering wind with time
Temperature	Variable decreases as well as increases	
Rain rate	Variable from high to no precipitation	

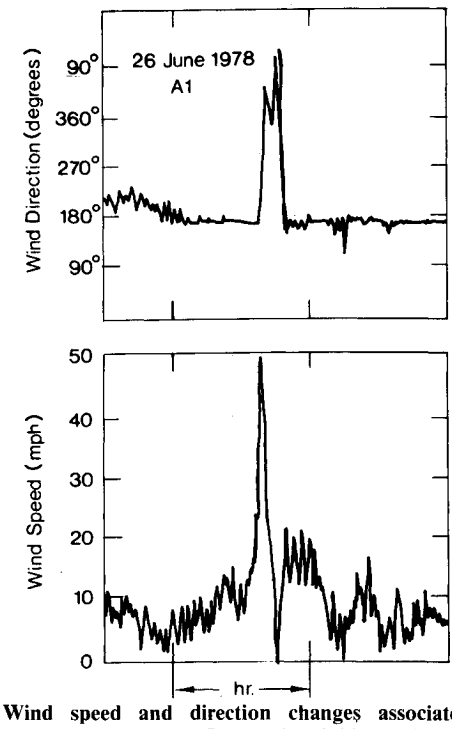

Fig. 4 Wind speed and direction changes associated with a microburst measured at Dulles International Airport (after Bedard et al.[4]).

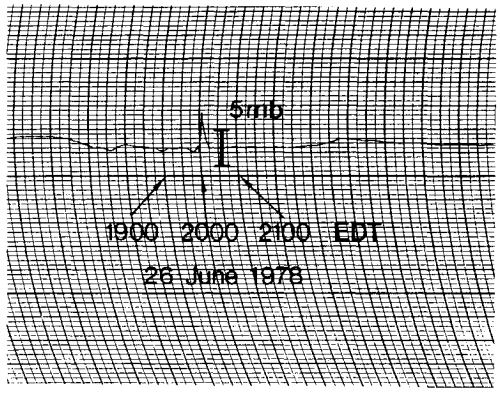

Fig. 5 Pressure nose associated with the microburst measured at Dulles Airport (after Bedard et al.[4]).

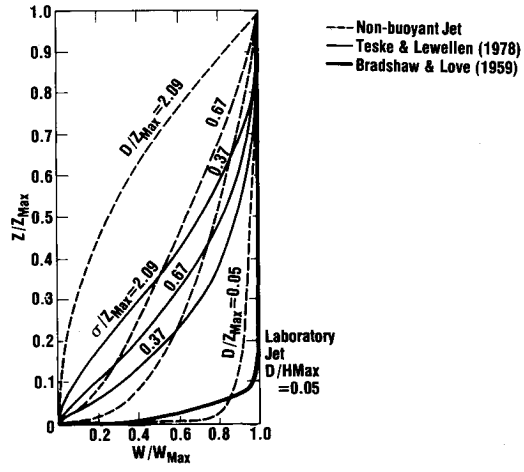

Fig. 6 Numerical and experimental results for downflow speed as a function of height compared with speed changes calculated from Eq. (1).

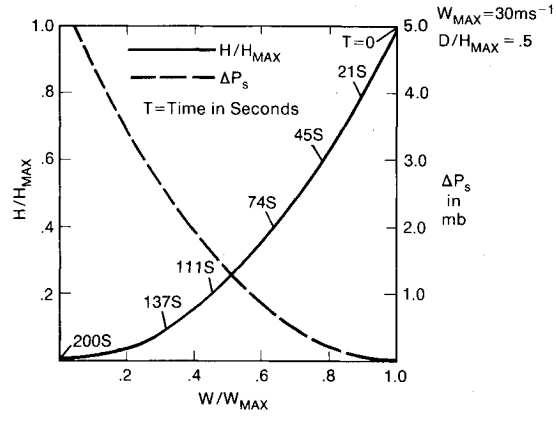

Fig. 7 Downflow speed and stagnation pressure as a function of height and time assuming $W_{max} = 30\ ms^{-1}$ and $\sigma/H_{max} = 0.5$.

the lack of downflow data is caused by the smaller areas covered by downflow regions relative to gust fronts. For example, a gust front propagating radially outward 20 km from a downflow source region 3 km wide covers over 1000 km^2, compared with the ~5 km^2 source region. In practice, downflow translation (typically at 10 ms^{-1}) could cover about 30 km^2, making the disparity not as great. Byers[8] notes that the scale size of pressure nose measurements is usually less than 5 miles. Furthermore, in terms of lifetime, an active gust front can persist for over 30 min, contrasted with a downflow lifetime of less than 10 min. Another reason for lack of data for thunderstorm downflows, particularly at lower altitudes, is the caution exercised by probe aircraft traversing thunderstorms at high enough levels to insure safety. All of these factors combine to make documented cases of intense downflows relatively rare. Data from the JAWS experiment should expand the existing data base.

Caracena and Kuhn[9] analyzed data from the Thunderstorm Project,[10] finding an average downflow width of about 1.7 km and a most probable width of 1 km. Fujita,[11] estimating downflow widths and path lengths from damage patterns, observed a wide range of widths (from less than 0.5 to more than 10 miles in diameter). Faust[7] documented one case having a width of about 100 m.

Based upon the path lengths observed by Fujita,[11] we estimate a range of lifetimes from less than 100 s to over 15 min with the wider downflows tending to have longer lifetimes. A translation speed of 10 ms^{-1} is assumed in making these estimates and surface damage is asumed to occur only near the periphery of the downflow. Obtaining data concerning downflow lifetimes is another area requiring more direct experimental measurements. The short time intervals possible have not been well resolved by most experiments.

The Thunderstorm Project[10] remains an exceptional resource for specifying thunderstorm properties. Fujita and Byers[6] present Thunderstorm Project data showing downdraft speed as a function of height. With the exception of the Doppler radar data of Strauch and Merrem,[12] there are few published measurements of downflow speed as a function of height in the literature. This is an indication of the caution with which pilots view downflow portions of severe thunderstorms and an index of the difficulties in measuring such a concentrated, transient system.

Bases for Analytical Representation of a Thunderstorm Downflow/Outflow System

Asnani[13] developed an analytical expression for a thunderstorm downflow and outflow. Sweezy et al.[14] also produced expressions for simulating thunderstorm flowfields.

A problem is to assign values to constants in these expressions and to insure that the computed flows adequately represent thunderstorms. Expressions for the downburst vertical speed as a function of height and radius must be obtained and inserted in the continuity equation.

We can simulate the data for the variation of W with height for a range of ratios of a characteristic width σ to a source height Z_{max} as a combination of dimensionless parameters. Using the expression

$$\frac{W}{W_{max}} = \left[\frac{Z}{Z_{max}}\right]^{\sigma/Z_{max}} \tag{1}$$

we can obtain an approximation to the experimental data over a range of σ/Z_{max}. Figure 6 shows a plot of this expression together with data from Teske and Lewellen[15] and data for a laboratory jet. Equation (1) ignores the buoyancy forces, implying that a nonbuoyant jet can indicate the relative importance of buoyancy forces along the downflow path. It is certainly reasonable that downflow jets of smaller diameter will approach the surface more closely, but at lower levels the nonbuoyant expression predicts higher downflow speeds than expected from available experimental data or numerical work of Teske and Lewellen.[15] Loss of negative buoyancy at low altitudes can explain this.

Because of the complexities of downflows—including entrainment, detrainment, condensation, evaporation, and adiabatic heating, all varying with position along the downflow—much work is required to provide more exact guidance concerning the parameters controlling these flows. The relatively simple Eq. (1) seems to provide a reasonable simulation of thunderstorm downflow W vs height profiles (when the downflow diameter is less than the source height). Such expressions (which ignore much of the important physics of downflow processes) can nevertheless serve as the basis for simple calculations illuminating the basic properties of downflows and provide a means of modeling downflows for simulations of aircraft response.

The Position of the Leading Edge of a Downflow and the Surface Stagnation Pressure as a Function of Time

Assuming that the steady-state downflow profile also reflects the time-height history of the leading edge of a downflow, we can use Eq. (1) to estimate the position of a parcel of air and the stagnation pressure as a function of time. Thus we obtain the relation

$$T = \frac{Z_{max}^{\sigma/Z_{max}}}{W_{max}(1-\sigma/Z_{max})}\left(Z_{max}^{1-\sigma/Z_{max}} - Z^{1-\sigma/Z_{max}}\right) \tag{2}$$

where T is the time the flow takes to move from Z_{max} to any height above the surface of the Earth. We compute the stagnation pressure from the reduction in W at a given height. Figure 7 shows the results for $W_{max} = 30$ ms^{-1}. One significant point is that we predict detectable pressure rises at the surface over 1 min prior to the arrival of the downflow air near the surface.

For more complete three-dimensional simulations of downflow/outflow systems, the ratio σ/Z_{max} can set the form of these equations. For example, in the relations of Asnani,[13] we find his expressions for the horizontal wind speed beneath the downflow become the following:

For $r \le R$,

$$U = \frac{W_{max}}{2\rho}\left[\frac{r}{R}\left(\frac{1}{2} - \frac{1}{N+2}\left(\frac{r}{R}\right)^N\right)\right]\left[\frac{Z}{Z_{max}}\right]^{Z_{max}/\sigma - 1} \tag{3}$$

and for $r > R$,

$$U = \frac{W_{max}}{2\rho}\left[\frac{r}{\rho}\frac{N}{2(N+2)}\right]\left[\frac{Z}{Z_{max}}\right]^{Z_{max}/\sigma - 1} \tag{4}$$

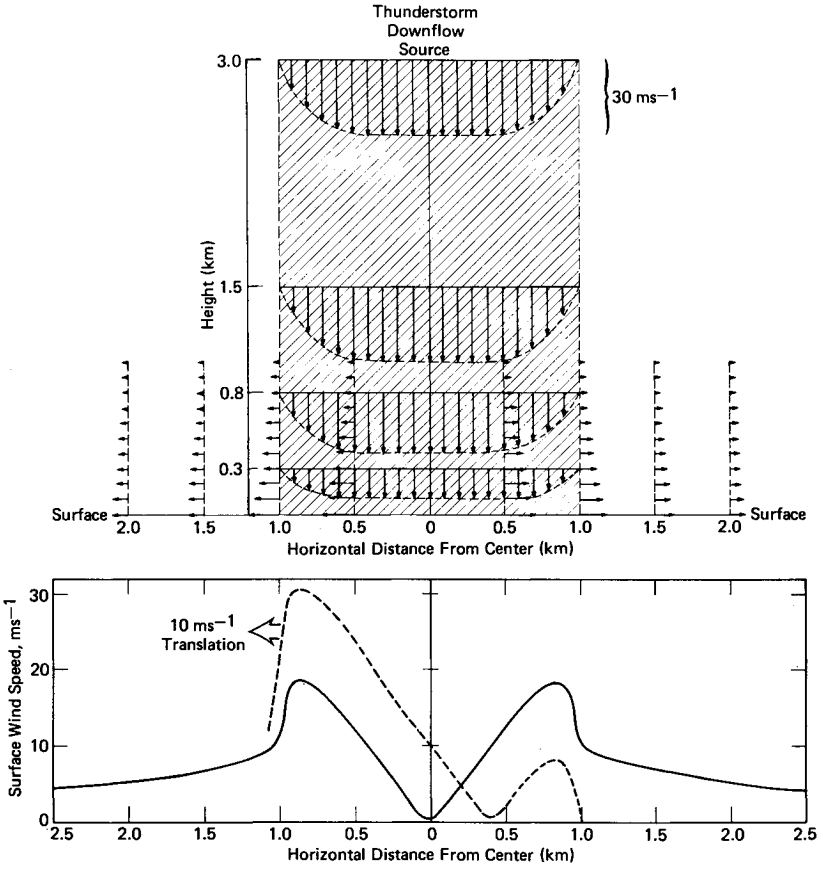

Fig. 8 Computed thunderstorm downflow/outflow vectors. Also shown are the surface speed changes with and without an assumed translation for the system.

where Asnani defined Z as the vertical distance from the source R the radius of the downflow r the radial distance from the center of the downflow, N a constant determining the variation of W from the center of the jet, and ρ the air density This expression ignores surface friction effects

Setting $N=10$ simulates a downflow jet with the W vs r profile shown in Fig 8 Assuming a σ/Z_{max} ratio of 0 2, $Z_{max}=3$ km, and $W_{max}=20$ ms^{-1}, we obtain the W vs height flows and the horizontal wind field shown in Figure 6. Horizontal surface wind beneath the downflow (Fig 8) shows a minimum just beneath the downflow center If a translation speed is added to this profile, the form of the outflow (also shown in Fig 8) can explain the tree-fall patterns described by Fujita [11]

While not directly addressing the important physics of the microburst, such expressions can nevertheless provide a valuable model for simulations of downburst effects The downflow width, radial variation of W in the source region, and the vertical variation of W with height above the surface may all be adjusted In spite of the value of such flexible representatives of downbursts for simulation testing (e g , aircraft response), a remaining need is to understand the physics of the downflow no matter how well represented by semiempirical approachs

Vorticity and Thunderstorm Microbursts

Models of downflow systems predict smaller vertical speeds for the smaller diameter systems because of the effects of entrainment It is difficult to determine the relative im portance of initial momentum and negative buoyancy forces based upon the available data Furthermore, it is not clear what role vorticity plays in the mass transfer process [16] Photographs of impacting microbursts show evidence of strong circulations near the leading edge [17]

Strong circulations could be generated by the initial formation process or formed by strong shear layers at the discontinuity of the descending downdraft Such circulations could be important not only in transferring air from upper to lower levels, but in determining how the diverging air moves in the near surface layer In addition the choice of optimum remote sensor type and processing for detection and study of microbursts can also depend upon the strength and orien tation of centers of vorticity Past studies have emphasized important larger scales in the thunderstorm complex There is also a need for an experimental program addressing the smaller (10 100 m) scales that are important for un derstanding the dominant physical processes and may have implications for guiding detection and warning approaches

Thunderstorm Microbursts— A Suggested Detection Approach

Probably the most dangerous location for a microburst impact is on a runway or in an approach zone In such situations, the diverging flows from even quite small microbursts can produce the increasing/decreasing lift couplet that is so difficult to recover from at low altitudes For this reason, it seems advisable to give priority to providing downburst detection along runway and in approach zones

Although there is evidence that dangerous microbursts on scales of 100 200 m do occur,[7] little is known about these smaller scales Such small scale systems may be hazards to general aviation even if the area over which strong divergence occurs should be too limited to be dangerous to large aircraft Experiments to date have addressed the larger spatial scales

An effective and practical system can be built around an expanded version of the present LLWSAS system. Expansion to a relatively sparse array of anemometers (e g , 10) would be an improvement, but would not provide the coverage required However, each anemometer site could serve as a secondary collection point for a local extension of the system If simple yes/no types of sensors are applied (e g., pressure jump detectors[18] or wind threshold detectors,[19] the one bit data can be effectively processed at low cost with minimum inpact on the data acquisition and processing system

The Stapleton Airport system is used in the example (Fig 9) showing the form such a system could take The LLWSAS is expanded from five to nine outer sites Also, existing sites are used as data collection points for lines of pressure and wind threshold sensors providing coverage from the runways and approach zones This configuration takes into account a generally west to east motion observed for many microbursts during the JAWS project

Representativeness of Flows Aloft—The Effects of Near-Surface Stable Layers

The near surface stability can be an important factor in determining how well a flowfield is represented by surface shears Data from the Dulles Airport experiment provided reference measurements in the lowest several hundred meters for comparison with a dense array of surface sensors Figures 10 and 11 indicate that density current strengths can be un derestimated by surface sensors Pressure sensors responding to the integrated fields aloft and providing propagation speeds can still provide a detection capability

Figure 10 presents monostatic acoustic sounder data in which the top of the dark return at about 300 m probably marks the top of an inversion layer. A rawinsonde ob servation at 1900 EDT shows the presence of an inversion At about 2110 EDT, a disturbance with a wave like structure at the leading edge appears above the inversion layer We in terpret this discontinuity as an atmospheric density current Doppler sounder profiles indicate a wind vector change in excess of 10 ms^{-1} at 500 m accompanying the density current The wind shear between the surface and 300 m also indicates the presence of the stable layer

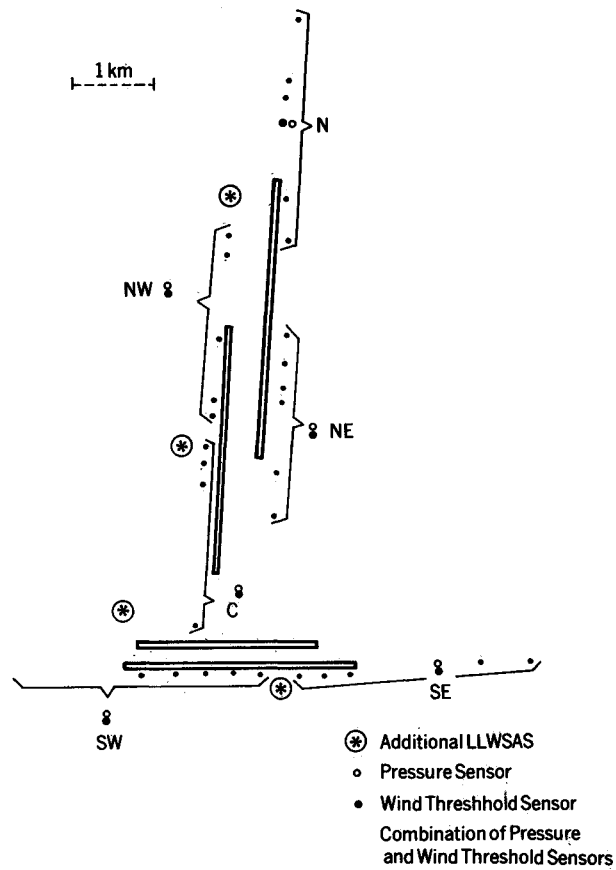

Fig 9 A suggested terminal airport configuration for microburst and gust front detection

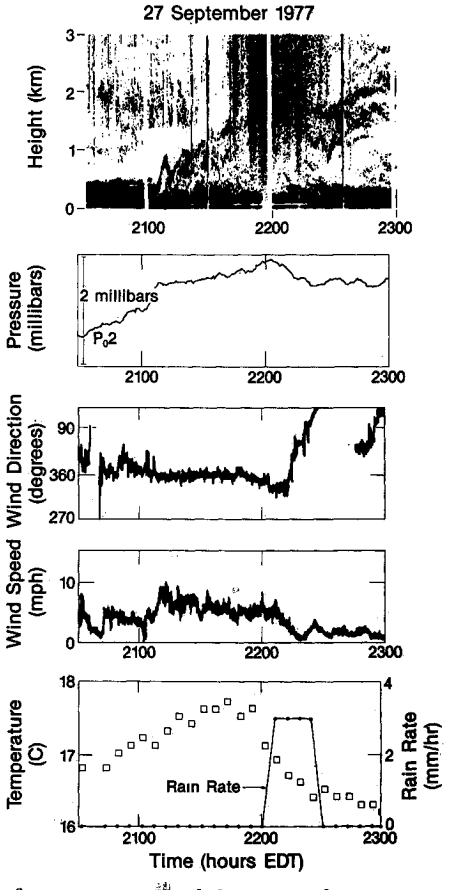

Fig. 10 Surface measurements below a gust front propagating on a surface-based inversion.

Figure 10 shows monostatic acoustic sounder data together with surface observations of temperature, rain rate, wind speed, wind direction, and pressure, all adjusted to a common time scale. The temperature shows an increase associated with the leading edge of the density current rather than the expected decrease. The increase in rain rate occurring later in the event probably results from a separate source region moving from a different direction. A minor increase in wind speed and a significant rise in pressure accompany the leading edge of the discontinuity. The form of the surface pressure trace is a representation of the form of the density current aloft. This is because an important component of the pressure field results from the integrated density changes in the column of air above the sensor. Data from pressure sensor near the monostatic sounder show the perturbation at the leading edge. This situation is described in more detail by Bedard and Sanders.[20]

As indicated previously, an additional element of concern for microbursts is the importance of vorticity for the radial flowfields produced near the surface. By analogy with the way the aircraft wing tip vortices and experimental-scale model vortices move in ground effect, the influences of surface shear layers can be expected to cause any centers of vorticity to rise above the surface. Not enough is known about the importance of vorticity in microburst dynamics to make concrete estimates in this regard. There have been qualitative observations of smoke-ring-like appearances of microbursts near the surface from the entrained dust. The concern should be that the leading edges of microburst outflows could rise high enough so that surface sensors would not detect them.

Sources of False Alarms

False alarms can fall into two classes, instrumental and physical. Examples of instrumental false alarms for pressure detectors can be caused by thermal effects, wind-induced

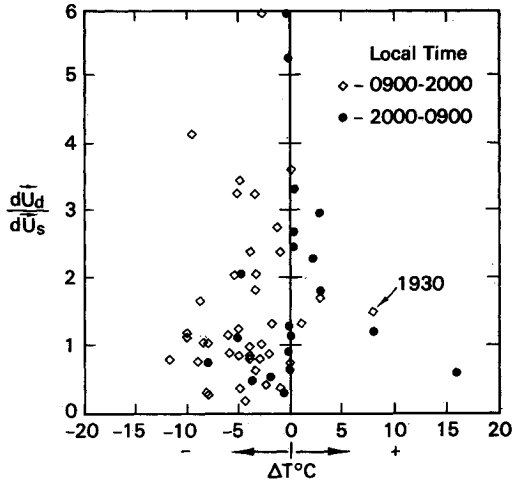

Fig. 11 Summary of data showing the ratio of maximum wind vector measured aloft for gust fronts to wind vector measured at the surface, as a function of the temperature change associated with the system.

pressures, and noise in communications links. These problems of execution have been solved by system redesign and/or processing techniques. Bedard et al.[4] review the various problems found during the application of an extensive system of pressure sensors at Dulles Airport, describing solutions to the instrumentation problems identified.

Sources of physical false alarms for pressure sensors were addressed in studies by Bedard and Cairns[21] and Bedard et al.[4] Gravity shear waves at tropopause heights accounted for most false alarms (about 13% during a 4 yr period at O'Hare Airport, 4% during the summer months). Pressure changes from unknown sources accounted for 14% of the total. In an airport environment, the transfer of the weight of the aircraft to the surface of the Earth can cause large (>1 mb) pressure changes. Fortunately, these are of short duration (1-2 s) and should be easily discriminated against.

A parallel set of false alarm sources exists for wind sensors. Preliminary results from analysis of the LLWSAS system operated during the JAWS experiment indicate that local flows of small scale account for many alarms observed during JAWS. Sporadic changes during daytime convection produced a large proportion of these. During the Dulles and JAWS experiments, short-term disturbances of the nocturnal boundary layer also produced sufficient wind vector changes to cause alarms. These types of shear, because of both their limited height and horizontal extent, are unlikely to represent a hazard. When pressure and wind sensors are combined, their complementary nature permits and additional level of discrimination. This should permit system designs with lower total false alarm rates and improved detection capabilities.

Conclusions

Reviews of properties of thunderstorm gust fronts and microbursts provide bases for evaluating the strengths and weaknesses of various surface sensors for the detection of wind shear from thunderstorms. The direct measurement of gust front wind shears by anemometers can be complemented by pressure measurements that often provide additional warning times of 1-2 min. Such precursor pressure increases can occur from vertical accelerations of air in front of the density current.

For microburst detection, combined anemometer/pressure sensing offers similar advantages. A large pressure increase directly beneath a descending downflow provides a detection method in the stagnation region where only small wind speeds may occur. Calculations indicate an additional warning time (>1 min) could be provided by the pressure field increase beneath a descending microburst. A possible configuration

for such a combined anemometer/pressure sensor system appears in Fig 9 Because of the small time (minutes) and space scales (often <1 km) involved with thunderstorm microbursts, warning lead times of tens of seconds can be critical to operations. Combined anemometers and pressure sensors in more dense arrays should improve warnings to pilots

References

[1]Goff, R C , "The Low Level Wind Shear Alert System (LLWSAS) " FAA RD 80-45, 1980 120 pp

[2]Bedard A J Jr ' Sources and Detection of Atmospheric Windshear, ' *AIAA Journal* Vol 20 1982 pp 940 945

[3]Charba, J., "Application of Gravity Current Model to Analysis of Squall line Gust Front ' *Monthly Weather Review* Vol 102 1974 pp. 140 156

[4]Bedard, A J Jr , Merrem, F H Simms, D. and Cairns M M A Thunderstorm Gust Front Detection System Part I: System Operation and Significant Case Studies; Part II: Statistical Results FAA RE 79-55, 1979 130 pp.

[5]Wakimoto R. M ' The Life Cycle of Thunderstorm Gust Fronts as Viewed with Doppler Radar and Rawinsonde Data, *Proceedings of 12th Conference on Severe Local Storms* Jan 12-15 1982, San Antonio Texas, American Meteorological Society 1982, pp 409 412

[6]Fujita, T. T., and Byers, H R , "Spearhead Echo and Downburst in the Crash of an Airliner ' *Monthly Weather Review* Vol 105 1977, pp 129-146.

[7]Faust H., 'Untersuchungan von Forstschaden hinsichtlich der windstruktur bei einer ' *Meteorologische Rundschau* Vol 1 1941 pp. 290 297

[8]Byers H. R , *Compendium of Meteorology,* American Meteorological Society, Boston, 1951

[9]Caracena F and Kuhn P M Remote Sensing Thunderstorm Outflow Severity with an Airborne IR Sensor *Conference on Weather Forecasting and Analysis and Aviation Meteorology* Oct 16-19 Silver Spring Md American Meteorological Society Boston 1978, pp 287 292

[10]Byers, H. R and Braham R R , The Thunderstorm, Govern ment Printing Office, Washington D C 1949 287 pp

[11]Fujita T T Manual of Downburst Identification for Project NIMROD, Dept of the Geophysical Sciences University of Chicago, Chicago Satellite and Mesometeorology Research Paper 156 1978, 104 pp

[12]Strauch, R G and Merrem, F H 'Structure of an Evolving Hailstorm Pt III: Internal Structure from Doppler Radar *Monthly Weather Review* Vol 104 1976 pp 588 595.

[13]Asnani G C Theoretical Model of Thunderstorm Winds near the Ground ' *Indian Journal of Meteorology and Geophysics* Vol 12 1961 pp 7 13

[14]Sweezy W B Moninger W R , and Strauch R G Simulation of Radar-Measured Doppler Velocity Profiles in Low Level Wind Shear (Phase I), NOAA/ERL Wave Propagation Laboratory Boulder Colo , Final Report FAA RD-78 46 to the Federal Aviation Administration 1978

[15]Teske M E and Lewellen W S The Prediction of Tur bulence and Wind Shear Associated with Thunderstorm Gust Fronts *Conference on Atmospheric Environment of Aerospace Systems and Applied Meteorology* Nov 14 16, New York American Meteorological Society Boston 1978 pp 140 147

[16]Caracena, F Is the Microburst a Large Vortex Ring Imbedded in a Thunderstorm Downdraft? Paper presented at Fall Meeting of American Geophysical Union, San Francisco 1982

[17]Fujita, T T and Wakimoto R. M JAWS Microbursts Revealed by Triple-Doppler Radar, Aircraft and PAM Data *13th Conference on Severe Local Storms,* Oct 17 20, Tulsa Okla American Meteorological Society Boston 1983 pp 97 100

[18]Bedard A J Jr and Meade, H B. The Design and Use of Sensitive Pressure Jump Sensors to Detect Thunderstorm Gust Fronts Part I: Pressure-Jump Detector Design ' *Journal of Applied Meteorology* Vol 16, 1977, pp 1049-1055

[19]Bedard A J Jr. and Fujita, T T , 'An Omnidirectional Tilt Insensitive, Wind Speed Threshold Detector *Proceedings at 4th Symposium on Meteorological Observations and Instrumentation* April 10-14 Denver American Meteorological Society Boston 1978 pp 83 86.

[20]Bedard A J Jr and Sanders, M J Jr Thunderstorm Related Wind Shear Detected at Dulles International Airport Using a Doppler Acoustic/Microwave Radar a Monostatic Sounder and Arrays of Surface Sensors *Conference on Weather Forecasting and Analysis and Aviation Safety* Oct 16 19 1978 Silver Spring Md American Meteorological Society Boston 1978 pp 347 352

[21]Bedard A J Jr and Cairns, M M. "Atmospheric Pressure Jumps Measured with Arrays of Sensitive Pressure Sensors in the Vicinity of Chicago s O Hare International Airport NOAA Tech Memo ERL WPL 28 1977 p 29

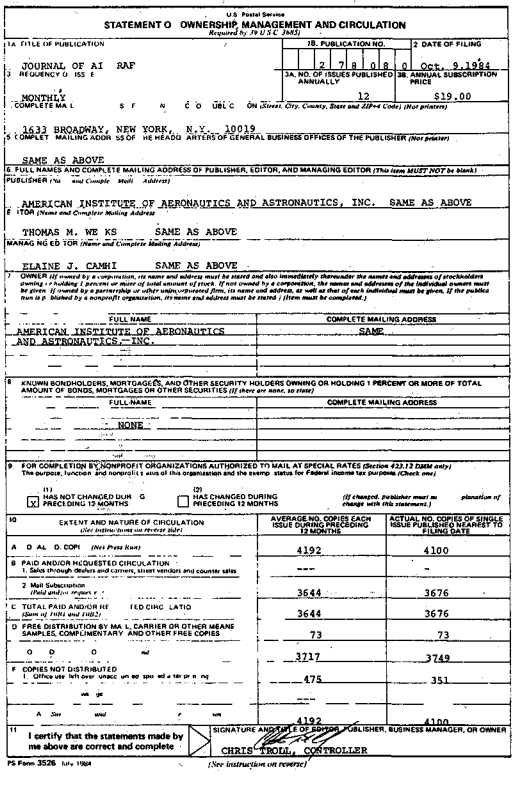

U.S. Postal Service

STATEMENT O OWNERSHIP, MANAGEMENT AND CIRCULATION

Required by 39 U.S.C. 3685)

1A. TITLE OF PUBLICATION	1B. PUBLICATION NO.	2. DATE OF FILING
JOURNAL OF AI RAF	2 7 8 0 8 0	Oct. 9,1984
3. FREQUENCY O ISS E	3A. NO. OF ISSUES PUBLISHED ANNUALLY	3B. ANNUAL SUBSCRIPTION PRICE
MONTHLY	12	$19.00

4. COMPLETE MAILING ADDRESS OF KNOWN OFFICE OF PUBLICATION (Street, City, County, State and ZIP+4 Code) (Not printers)

1633 BROADWAY, NEW YORK, N.Y. 10019

5. COMPLETE MAILING ADDRESS OF HEADQUARTERS OF GENERAL BUSINESS OFFICES OF THE PUBLISHER (Not printer)

SAME AS ABOVE

6. FULL NAMES AND COMPLETE MAILING ADDRESS OF PUBLISHER, EDITOR, AND MANAGING EDITOR (This item MUST NOT be blank)

PUBLISHER (Name and Complete Mailing Address)

AMERICAN INSTITUTE OF AERONAUTICS AND ASTRONAUTICS, INC. SAME AS ABOVE

EDITOR (Name and Complete Mailing Address)

THOMAS M. WE KS SAME AS ABOVE

MANAGING EDITOR (Name and Complete Mailing Address)

ELAINE J. CAMHI SAME AS ABOVE

7. OWNER (If owned by a corporation, its name and address must be stated and also immediately thereunder the names and addresses of stockholders owning or holding 1 percent or more of total amount of stock. If not owned by a corporation, the names and addresses of the individual owners must be given. If owned by a partnership or other unincorporated firm, its name and address, as well as that of each individual must be given. If the publication is published by a nonprofit organization, its name and address must be stated.) (Item must be completed.)

FULL NAME	COMPLETE MAILING ADDRESS
AMERICAN INSTITUTE OF AERONAUTICS AND ASTRONAUTICS, INC.	SAME

8. KNOWN BONDHOLDERS, MORTGAGEES, AND OTHER SECURITY HOLDERS OWNING OR HOLDING 1 PERCENT OR MORE OF TOTAL AMOUNT OF BONDS, MORTGAGES OR OTHER SECURITIES (If there are none, so state)

FULL NAME	COMPLETE MAILING ADDRESS
NONE	

9. FOR COMPLETION BY NONPROFIT ORGANIZATIONS AUTHORIZED TO MAIL AT SPECIAL RATES (Section 423.12 DMM only)

The purpose, function and nonprofit status of this organization and the exempt status for Federal income tax purposes (Check one)

(1) [X] HAS NOT CHANGED DUR G PRECEDING 12 MONTHS

(2) [ ] HAS CHANGED DURING PRECEDING 12 MONTHS

(If changed, publisher must su planation of change with this statement.)

10. EXTENT AND NATURE OF CIRCULATION (See instructions on reverse side)	AVERAGE NO. COPIES EACH ISSUE DURING PRECEDING 12 MONTHS	ACTUAL NO. COPIES OF SINGLE ISSUE PUBLISHED NEAREST TO FILING DATE
A. TOTAL NO. COPIES (Net Press Run)	4192	4100
B. PAID AND/OR REQUESTED CIRCULATION 1. Sales through dealers and carriers, street vendors and counter sales	---	-
2. Mail Subscription (Paid and/or requested)	3644	3676
C. TOTAL PAID AND/OR REQUESTED CIRCULATION (Sum of 10B1 and 10B2)	3644	3676
D. FREE DISTRIBUTION BY MAIL, CARRIER OR OTHER MEANS SAMPLES, COMPLIMENTARY, AND OTHER FREE COPIES	73	73
E. TOTAL DISTRIBUTION (Sum of C and D)	3717	3749
F. COPIES NOT DISTRIBUTED 1. Office use, left over, unaccounted, spoiled after printing	475	351
2. Return from News Agents	---	---
G. TOTAL (Sum of E, F1 and 2 - should equal net press run shown in A)	4192	4100

11. I certify that the statements made by me above are correct and complete

SIGNATURE AND TITLE OF EDITOR, PUBLISHER, BUSINESS MANAGER, OR OWNER

CHRIS TROLL, CONTROLLER

PS Form 3526 July 1984 (See instructions on reverse)